

## Castanea sativa Mill. plantations as a low-carbon landslide hazard mitigation measure

Ana Sofia Dias, Alexia Stokes, Gianfranco Urciuoli

► **To cite this version:**

Ana Sofia Dias, Alexia Stokes, Gianfranco Urciuoli. Castanea sativa Mill. plantations as a low-carbon landslide hazard mitigation measure. 2nd International Conference on Energy Geotechnics (ICEGT 2020), International Society for Soil Mechanics and Geotechnical Engineering (ISSMGE), Sep 2020, La Jolla, California, USA, United States. pp.12003, 10.1051/e3sconf/202020512003 . hal-03018831

**HAL Id: hal-03018831**

**<https://hal.inrae.fr/hal-03018831>**

Submitted on 23 Nov 2020

**HAL** is a multi-disciplinary open access archive for the deposit and dissemination of scientific research documents, whether they are published or not. The documents may come from teaching and research institutions in France or abroad, or from public or private research centers.

L'archive ouverte pluridisciplinaire **HAL**, est destinée au dépôt et à la diffusion de documents scientifiques de niveau recherche, publiés ou non, émanant des établissements d'enseignement et de recherche français ou étrangers, des laboratoires publics ou privés.



# ***Castanea sativa* Mill. plantations as a low-carbon landslide hazard mitigation measure**

Ana Sofia Dias<sup>1,2,3\*</sup>, Alexia Stokes<sup>1</sup>, Marianna Pirone<sup>2</sup>, and Gianfranco Urciuoli<sup>2</sup>

<sup>1</sup>AMAP, INRAE, University of Montpellier, IRD, CNRS, CIRAD, 34000 Montpellier, France

<sup>2</sup>DICEA, University of Naples Federico II, Via Claudio 21, 80125 Napoli, Italy

<sup>3</sup>Department of Engineering, Durham University, Lower Mountjoy, DH1 3LE Durham, UK

**Abstract.** In the last twenty years, several rainfall-induced landslides occurred in areas surrounding Mount Vesuvius (Campania, Italy). Landslides usually involve the shallow pyroclastic soil layers (2-3 m thick) covering the steep slopes of the Lattari Mountains. The cultivation of trees for fruit production on the pyroclastic cover is a common practice by local farmers. Woody vegetation contributes to slope stability through the mechanical reinforcement of soil by roots. We investigated the use of Sweet chestnut (*Castanea sativa* Mill.) trees as a low-carbon landslide mitigation measure to be applied in large areas where conventional geotechnical engineering solutions would be costly and extremely invasive, in order to respond to the demand in energy and environmental geotechnics for eco-friendly approaches. The root distribution of *C. sativa* in terms of root volume ratio was determined from soil cores. The mechanical reinforcement of soil by tree roots was quantified based on root-soil interaction models. Slope stability was analysed by means of limit equilibrium analyses performed on an infinite slope. The safety factor calculated for a cultivated slope was higher than for a fallow slope due to the mechanical reinforcement provided by roots. Therefore, the cultivation of *C. sativa* is a useful mitigation measure against shallow landslides.

## **1 Introduction**

The construction industry is responsible for a large fraction of carbon emissions resulting from human activity. Nowadays, the development of low-carbon solutions is a priority for the society and, hence, for energy and environmental geotechnical engineers. Soil reinforcement through plant root systems represents a low-carbon strategy used to tackle slope instability [1].

Several flowslides occurred in the Campania region (Southern Italy) in recent years, such as Sarno (1998), Nocera (2005) and Ischia (2006), causing human and material losses. Generally, flowslides, debris flows, and debris avalanches occur during the wet season after prolonged intense rainfall events on steep slopes covered by a thin pyroclastic soil cover (1-2 m thick) resting on fractured limestone [2]. After the 1998 disaster, slopes and foothills of Pizzo d'Alvano in Sarno and neighbouring municipalities were secured by the construction of massive geotechnical structures that were costly in terms of both financial and carbon footprint, in order to prevent the occurrence of a future similar incident. Nowadays, hazard mitigation measures characterized by low environmental impact are necessary.

Previous studies pointed out that flowslides in the Campania region are more frequent in shrublands than on slopes planted with Sweet chestnut (*Castanea sativa* Mill.) plantations [3]. However, Amato et al. [4]

suggested that fires and disturbance in the *C. sativa* plantations led to an increase in the risk of shallow landslides. Plants interact with slopes, not always in a positive way, by: (i) removing water from the soil through transpiration; (ii) preventing water infiltration through rainfall partition; and (iii) increasing rainfall infiltration through preferential flow channels created by roots. The most important contribution of woody vegetation, such as *C. sativa*, to slope stability is through the mechanical reinforcement of soil by root systems [5-7].

In order to engineer the use of *C. sativa* as a landslide mitigation measure, quantification of the reinforcement provided by the roots is required. We investigated the effect of *C. sativa* on slope stability by performing limit equilibrium analyses on an infinite slope. The contribution of both suction and mechanical effects of roots are taken into account in the calculation of soil shear strength. The apparent cohesion was estimated based on field measurements of suction and volumetric water content. The mechanical reinforcement of the soil exerted by roots was determined as a function of root volume ratio (RVR) quantified on site, and using data from soil cores.

## **2 Test site**

A site in Mount Faito, located in the Lattari Mountains (Campania, Southern Italy), was used as a case study.

\* Corresponding author: [ana.s.dias@durham.ac.uk](mailto:ana.s.dias@durham.ac.uk)

The test site was located on a slope facing North at approximately 850 m of altitude (40°40'32.29"N, 14°28'23.35"E). The mean slope angle of the test site is 26.5° with local angles ranging between 13.2° and 44.3°.

### 2.1 Vegetation

The local vegetation is composed of Sweet chestnut trees (*Castanea sativa* Mill.) cultivated by local farmers (Fig. 1). The understory is mainly composed of ferns (*Pteridium aquilinum*). Several shrub species are also present, such as *Rubus ulmifolius* and *Corylus avellana*. A survey on a population of 27 *C. sativa* individuals revealed that the mean diameter at breast height of the trees was 0.41±0.28 m and the tree density was 0.08 individuals per m<sup>2</sup>.

The groundcover dramatically changes throughout the year. All the understory is removed during the month of October by the local farmers to facilitate the collection of the fruits (chestnuts) from the ground. Leaf drop is at the end of November (*C. sativa* is a deciduous tree). Consequently, the only groundcover in the area is composed of litter (dry leaves, fruits and branches) until April when the vegetation starts to regrow, reaching its peak in July (Fig. 1).



**Fig. 1.** Dominant vegetation at the test site in Mount Faito (Campania, Southern Italy): mature *Castanea sativa* Mill., and ferns *Pteridium aquilinum* [7]. Photograph of 22/07/2016.

### 2.2 Stratigraphy, soil physical and mechanical properties

The stratigraphy of this site consists of three main groups of pyroclastic soil deposits (Fig. 2). The layers originated during explosive eruptions of Mount Vesuvius and probably Campi Flegrei [3]. The top layer is referred to as soil A, with a thickness of 0.80 m, and can be subdivided into soil A1 (0.35 m thick) and A2 (0.45 m thick). This soil, according to the USCS classification [8], varies between silty sand with gravel and silty gravel

with sand. A thick layer of pumices, referred as soil B, is present with a thickness of 1.20 m, classified as a well graded gravel with sand. The deepest soil layers are soils C, subdivided into soil C1 and C2, which are finer soil (sandy silt) originated from a much older eruption [9]. Soil C2 was not always identified. The bedrock in this location consists of fractured limestone and can be found at 2 to 3 m in depth.

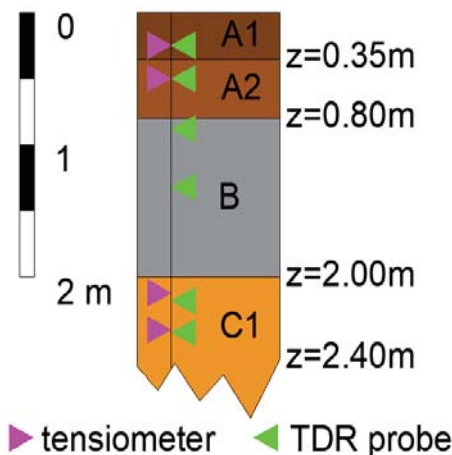


**Fig. 2.** Soil stratigraphy in Mount Faito test site and depth of installation of soil monitoring sensors (tensiometer and TDR probes).

The physical properties of the soil layers are reported in Table 1. These soils are characterized by a very high porosity, ranging between 0.64 and 0.80, similarly to the soil found in other test sites in Campania [2, 10-12].

**Table 1.** Soil physical and mechanical properties: specific gravity ( $G_s$ ), dry density ( $\rho_d$ ), porosity ( $n$ ), and soil friction angle ( $\phi'$ ) (adapted from Dias [7]; data for soil B are based on Papa et al. [10]).

Soil	$G_s$ (-)	$\rho_d$ (g cm <sup>-3</sup> )	$n$ (-)	$\phi'$ (°)
A1	2.606	0.918	0.643	36.5
A2	2.688	0.819	0.694	36.5
B	2.550	0.490	0.800	40.0
C1	2.656	0.735	0.722	32.1

Regarding the soil strength properties, direct shear tests were performed on undisturbed soil samples of soils A1 and C1 under fully saturated conditions. Soil cores were collected from horizontal boreholes on the sides of a road cut at the test site and the soil specimens for direct shear testing had dimensions of 60x60x20 mm.

The tests were performed at three different final confining stresses: 25, 50 and 75 kPa. The initial confining stress was applied and the vertical displacements (settlements) were recorded for

approximately 24 hours. Then, the specimens were submerged with water and vertical displacements were registered. Some of the soil specimens were partially unloaded after saturation from 75, 150 and 225 kPa (initial confining stress) to 25, 50 and 75 kPa (final confining stress), respectively. Each step took between 24 and 48 hours. The failure phase was performed at a rate of  $0.005 \text{ mm min}^{-1}$  allowing the shearing phase to be performed under drained conditions. A total of seven tests were performed for each soil.

The initial porosity of the tested samples varied between 0.61 and 0.80 in soil A1 and between 0.58 and 0.73 in soil C1. The results of these tests showed that soils A1 and C1 had a friction angle of  $36.5^\circ$  and  $32.1^\circ$ , respectively (Table 1). None of the soils showed a failure envelope characterised by an effective cohesion [7].

### 3 Field measurements

#### 3.1 Suction and water content

Suction and volumetric water content (vwc) were measured at the test site over two years (March 2017-March 2019) at different depths along the profile (Fig. 2). Suction was measured using Jet fill and SDEC France tensiometers, characterized by a range of measurements from 0 to 80 kPa. Tensiometers were installed at the test site ensuring good contact between the soil and the porous stone. The volumetric water content was determined based on measurements of the soil dielectric permittivity using TDR probes (time-domain reflectometry technique). The dielectric permittivity was then converted into volumetric water content according to the calibration relationships in Dias et al. [14].

The measurements were performed at three different dates along the hydrological year, corresponding to the three different phases of moisture distribution characteristic of this area (Fig. 3). The three periods were selected according to findings reported by Pirone et al. [13] and Urciuoli et al. [2]. Therefore, these measurements were used in the present study: (i) 20<sup>th</sup> December 2017, to investigate the response of the soil moisture distribution to the first rainfalls after the dry summer; (ii) 10<sup>th</sup> January 2018, as representative of wet period characterized by a constant distribution of water with depth and very low suction values; and (iii) 2<sup>nd</sup> May 2018, to detect the soil response to the growth of vegetation and temperature increase.

On 20 Dec, suction was lower at the surface then in soil C1 where suction was still decreasing as a response to the first rainfall events after the dry period (Fig. 3a). Therefore, the soil layer A ( $z < 0.5 \text{ m}$ ;  $s = 10\text{-}15 \text{ kPa}$ ;  $\text{vwc} = 0.4$ ) was wetter than soil C ( $z > 2.0 \text{ m}$ ;  $s = 50\text{-}60 \text{ kPa}$ ;  $\text{vwc} = 0.3\text{-}0.4$ ). On 10 Jan, a typical suction profile of the steady wet period ( $< 5 \text{ kPa}$ ) was observed, in which the suction was close to the air-entry value of these soils (approximately 6 to 12 kPa [21]) over the whole depth (Fig 3). In spring (2 May), the upper soil layer was drier than soil C (Fig. 3b) because evapotranspiration drove water into the atmosphere.

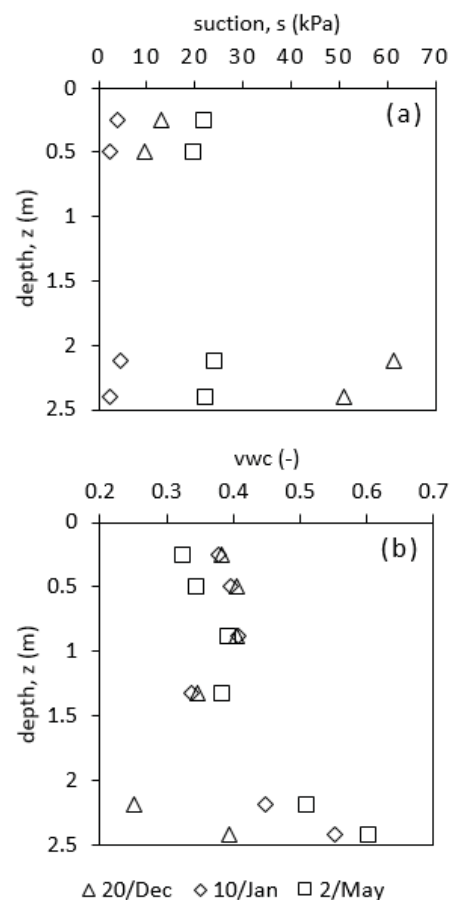


**Fig. 3.** Suction (a) and volumetric water content (vwc, b) over depth measured on 20 Dec 2017 ( $\Delta$ ), 10 Jan 2018 ( $\diamond$ ) and 2 May 2018 ( $\square$ ).

#### 3.2 Root vertical distribution on site

A borehole was made to collect a soil core with a diameter of 78 mm and a length of 1 m. Small soil samples were collected beyond 1 m of depth because it was not possible to collect intact samples. The soil core in the upper soil layer was collected at approximately 0.5 m from the installed instruments monitoring soil moisture in order to prevent disturbance of the instruments but being close enough to be representative of that soil profile. The borehole was refilled with the same type of soil collected elsewhere in the test site. The soil samples collected from soil B and C1 were obtained from the borehole where the TDR probes were installed without disturbing the soil where the probes were inserted. The samples of soil for the root quantification were of small dimensions and allowed the soil column above the sensors to be reconstituted.

The soil cores were divided into sections with a length of 100 mm. The roots were carefully collected from these soil samples with tweezers. The roots were displayed on a glass tray and scanned using an EPSON Perfection V700 Photo scanner. The collected images were analysed using the software WinRHIZO (Regent Instruments Inc.), which allows for the estimation of root volume per root diameter class. Therefore, the root

volume ratio (RVR), volume of roots per unit volume of soil, was estimated.

The roots were mostly found in the upper 0.20 m of the soil profile (RVR = 0.6 %). Then, the RVR decreased to 1.00 m deep, ranging from 0.1 to 0.3 %. The RVR in soils B and C1 was negligible because soil B had a low water storage capacity (Fig. 4). The trees' main source of water is rainfall, as the water table is found at the sea level. Soil had a low water storage capacity below 1 m in depth and so roots developed preferentially at shallow depths. Therefore, soil water content was not favourable for the growth of deep roots capable of anchoring the pyroclastic cover to the bedrock.

The estimated root density distribution is variable with depth. For example, the peak at 0.65 m (RVR=0.3%) was caused by a large number of roots in the root diameter class 3.5-4.0 mm (Fig. 4).

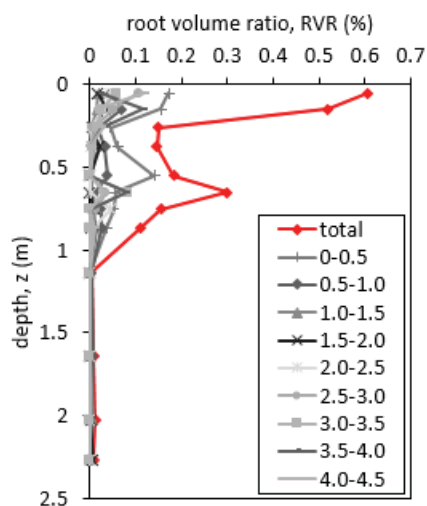


Fig. 4. Root volume ratio (RVR) distribution with depth grouped by root diameter classes from 0 to 4.5 mm and total RVR (red line).

#### 4 Estimation of the soil mechanical reinforcement by roots

The soil mechanical reinforcement due to roots depends on the tensile strength of the roots ( $T_r$ ) and on the root density.

The root tensile strength ( $T_r$ , in MPa) was estimated by a power-law based on the root diameter ( $d$ , in mm) and the two fitting parameters  $a$  and  $b$  (Eq. 1). Genet et al. [15] and Bischetti et al. [16] estimated the fitting parameters for roots of *C. sativa*. The relationship found by Bischetti et al. [16] was used here because it is more conservative than the relation obtained by Genet et al. [15]. The fitting parameters are  $a = 17.86 \text{ MPa mm}^{-1}$  and  $b = 0.53$ .

$$T_r = a d^b \quad (1)$$

The mechanical reinforcement provided by roots ( $\tau_{roots}$ ) is given by the generic Eq. 2, where  $k'$  is a parameter accounting for the different inclination of the

roots relative to the shear surface, and  $t_r$  is the tensile strength of root fibres per unit area of soil provided by a breaking model. Here,  $k'$  is assumed equal to 1 [17].

$$\tau_{roots} = k' t_r \quad (2)$$

Two different breaking models were adopted to estimate  $t_r$ : the Wu and Waldron model (WWM [18] and Waldron [19]); and the fibre bundle model (FBM [20]) following three different criteria of load distribution among roots: (i) equally among all intact roots (FBM<sub>numb</sub>), (ii) proportional to the cross-section area of the roots (FBM<sub>area</sub>), and (iii) proportional to the root diameter (FBM<sub>diam</sub>). In both models, the value of  $t_r$  is a function of  $T_r$  and of the root area ratio, assumed here equal to the RVR [21].

The mechanical reinforcement due to the roots along the depth is reported in Fig. 5. It presents a similar trend with depth observed in the root distribution (Fig. 4). The highest reinforcement was observed in the upper 0.2 m. The reinforcement peak at 0.5 m in depth was due to an increase in the RVR associated to roots in the diameter class 0-0.5 mm. On the other hand, the peak found at 0.65 m in the RVR due to roots in the class 3.5-4.0 mm does not correspond to an increase in reinforcement as large as the one caused by the 0-0.5 mm roots. The reinforcement below 1.0 m in depth was very low, as a result of low RVR.

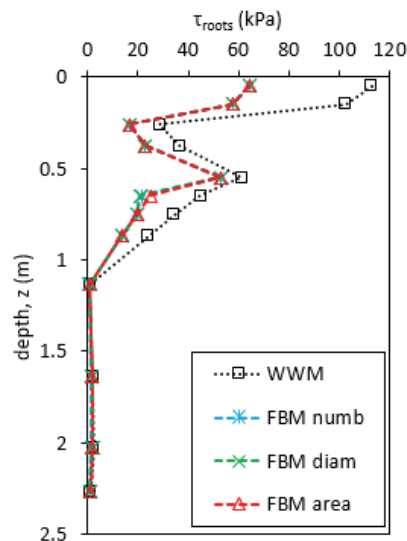


Fig. 5. Mechanical reinforcement due to the roots ( $\tau_{roots}$ ) against the depth estimated according to different models.

The reinforcement estimated by the WWM resulted in the highest values of  $\tau_{roots}$  as the model assumes that all roots break simultaneously, which is commonly a limitation of this model (Fig. 5) [20].

The estimations obtained by each of the load distribution criteria of the FBM are very similar among them. However, the criteria stating that the load is equally distributed among all intact roots (FBM<sub>numb</sub>) predicted the lowest values of mechanical reinforcement (up to 3.5 kPa lower than the other criteria at a given depth). Therefore, the reinforcement estimated by

FBM<sub>numb</sub> was adopted here in order to obtain conservative estimations of the safety factor.

The estimated  $\tau_{roots}$  values were approximately 60 kPa in the upper 0.2 m and at 0.5 m (due to the greater number of larger diameter roots). Overall, the reinforcement ranged between 20 and 40 kPa in the first meter of soil. In soils B and C1, the reinforcement ranged between 0.6 and 2.0 kPa. The values found here are in agreement with the ones reported by Bischetti et al. [16] for *C. sativa* in a forest in the North of Italy.

### 5 Slope stability

Slope stability was assessed by limit equilibrium analysis applied to an infinite slope characterized by soil stratigraphy reported in Fig.2. The safety factor (SF) was estimated by Eq. 3, where  $\tau_{soil}$  and  $\tau_{suction}$  are the soil's shear strength due to the soil friction angle and to suction, respectively, and  $\tau$  is the destabilizing stress. Eq. 3 can be elaborated into Eq. 4, where  $\alpha$  is the slope angle,  $S_r$  is the degree of saturation,  $s$  is the suction,  $\varphi'$  is the soil friction angle,  $\gamma$  is the soil unit weight, and  $z$  is the thickness of the soil layer above the chosen failure surface. In Eq. 4,  $\tau_{suction}$  was assumed equal to  $S_r \cdot s \cdot \tan \varphi'$ , therefore the Bishop effective stress approach was implicitly adopted with parameter  $\chi$  equal to the degree of saturation.

$$SF = (\tau_{soil} + \tau_{suction} + \tau_{roots}) / \tau \quad (3)$$

$$SF = (z\gamma \cdot \cos^2 \alpha \cdot \tan \varphi' + S_r \cdot s \cdot \tan \varphi' + \tau_{roots}) / (z\gamma \cdot \sin \alpha \cdot \cos \alpha) \quad (4)$$

The SF was calculated at three potential failure depths, in particular where the measurements of suction and volumetric water content were available: 0.25 m (soil A1); 0.55 m (soil A2); and 2.27 m (soil C1). The values of parameters adopted in the slope stability analyses are reported in Table 2. SF corresponding to three different dates over the year in the presence (roots) and absence of vegetation (bare) were determined (Fig. 6). The measurements reported in Fig. 3 were used to determine  $\tau_{suction}$  in Eq. 3. The presence of vegetation was taken into account by simply considering the root cohesion,  $\tau_{roots}$ .

**Table 2.** Soil parameters adopted in slope stability analyses: dry density ( $\gamma_d$ ), mechanical reinforcement provided by roots ( $\tau_{roots}$ ), and soil friction angle ( $\varphi'$ ).

Soil	$\gamma_d$ (kN m <sup>-3</sup> )	$\tau_{roots}$ (kPa)	$\varphi'$ (°)
A1	8.82	16.68	36.5
A2	8.46	52.56	36.5
B	4.80	-	-
C1	7.71	0.82	32.1

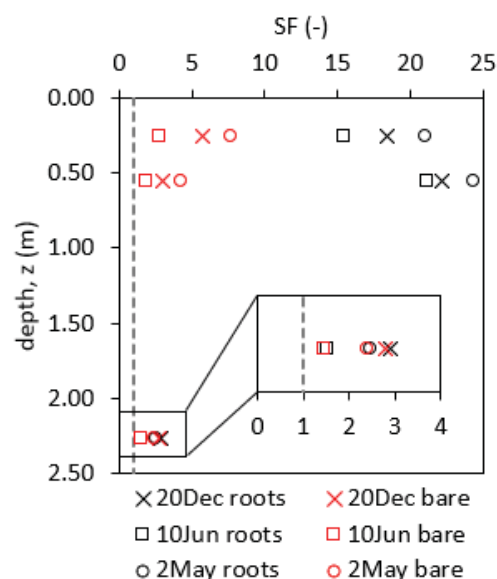


**Fig. 6.** Safety factor (SF) associated to the four potential failure surfaces assuming the presence of roots (roots) and disregarding it (bare) at three different dates over the year. The vertical dotted line represents the threshold of the minimum SF to guarantee the safety of the slope (SF=1).

In Fig. 6, the SF in presence of roots increased considerably at 0.25 and 0.55 m deep relative to the bare soil, due to the high density of roots at very shallow depths. The SF increased by 12 to 20 in soil A1 and A2. The SF in soil C1 increased by approximately 0.09 when the reinforcement by the roots was considered (corresponding to an increase of 3 to 6 %).

The lowest SF values establish on 10 Jan when suction is close to the air-entry value of the soil and water content is close to value at saturation [2]. The wet period is critical for the occurrence of landslides in this region because predisposing conditions in terms of suction distribution are met [23]. In case an intense rainfall occurs during this critical period, the uppermost soil layer (soil A) is susceptible to the sudden decrease in suction leading to a landslide. However, the roots of *C. sativa* can increase the SF of the layers more susceptible to landslides, moving the critical sliding surface to the deeper part of the soil cover, thus, requiring higher total rainfall to trigger flow slides than that predicted on bare slopes (Fig. 6).

The mechanical reinforcement of the soil exerted by roots was observed to be significantly higher than the contribution resultant from suction in the surficial layer at each date investigated (Fig. 7). The root contribution constitutes up to 86.6 % of the SF, while the soil friction angle and suction contribute to 9.6 and 29.6 %, respectively (Fig. 7). In soil C1, suction had a more relevant impact of the SF value as it decreased from 2.80 on 20/Dec (SF=2.80) to 1.44 on 10 Jan, in the case of bare soil (Fig. 6). In soil C1, the contribution of the roots represented up to 5.7 % of the SF, while the soil friction angle and suction contributed 82.0 % and 53.4 %, respectively, to the SF (Fig. 7).

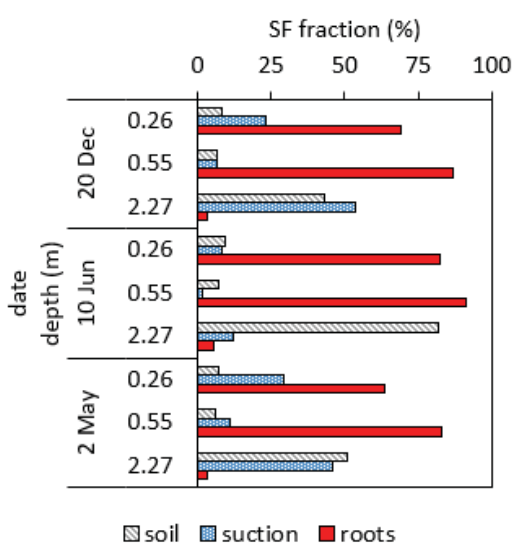


**Fig. 7.** Fraction of the safety factor (SF) in terms of percentage resulting from the contribution of the shear strength of the soil, by the suction and by the mechanical reinforcement due to the roots.

## 6 Conclusion

The root distribution of *C. sativa* in the test site in Mount Faito (Campania, Southern Italy) was investigated. We showed that the root density decreases greatly with depth. The root density was negligible below 1 m deep. This root distribution provided an increase in the shear strength of the root-permeated soil of up to 16.7 kPa in the upper most layer.

The reinforcement provided by the roots increased the SF at all the depths. However, the benefits of the presence of *C. sativa* roots were more significant in the surface soil layer A. Additionally, the mechanical reinforcement due to the roots was more significant than variations of SF caused by different moisture distributions along the year in the surficial layer. Root cohesion contributes to stabilise the topsoil and deepen the sliding surface.

In summary, the plantation of *C. sativa* enhanced slope stability and may be considered as a possible low-carbon landslide mitigation measure to be adopted, especially in the mitigation of shallow landslides (less than 1.0 m deep).

The authors wish to acknowledge the support of the European Commission via the Marie Skłodowska-Curie Innovative Training Networks (ITN-ETN) project TERRE 'Training Engineers and Researchers to Rethink geotechnical Engineering for a low carbon future' (H2020-MSCA-ITN-2015-675762).

## References

1. A. Tarantino, G. El Mountassir, S. Wheeler, et al., TERRE project: interplay between unsaturated soil mechanics and low-carbon geotechnical

- engineering, Proceedings of E-UNSAT Lisbon 2020 (to be published)
2. G. Urciuoli, M. Pirone, L. Comegna, L. Picarelli, Long-term investigations on the pore pressure regime in saturated and unsaturated sloping soils, *Eng Geol.* **212** (2016)
3. G. Di Crescenzo, A. Santo, Debris slides-rapid earth flows in the carbonate massifs of the Campania region (Southern Italy): Morphological and morphometric data for evaluating triggering susceptibility, *Geomorphology* **66** (2005)
4. M. Amato, P. Di Martino, G. Di Pasquale, et al., Il ruolo della vegetazione nella frana di Quindici, *Quaderni Di Geologia Applicata* **7**, 1 (2000)
5. A. Stokes, C. Atger, A. G. Bengough, T. Fourcaud, R. C. Sidle, Desirable Plant root traits for protecting natural and engineered slopes against landslides, *Plant Soil* **324** (2009)
6. J. H. Kim, T. Fourcaud, C. Jourdan, et al., Vegetation as a driver of temporal variations in slope stability: The impact of hydrological processes, *Geophys Res Lett.* **44**, 10 (2017)
7. A. S. R. A. Dias, The effect of vegetation on slope stability of shallow pyroclastic soil covers, PhD thesis, UNINA, UM (2019)
8. ASTM D 2487 – 17, Standard Practice for Classification of Soils for Engineering Purposes (Unified Soil Classification System) (2017)
9. G. Forte, M. Pirone, A. Santo, M. V. Nicotera, G. Urciuoli, Triggering and predisposing factors for flow-like landslides in pyroclastic soils: the case study of the Lattari Mts. (southern Italy), *Eng. Geol.* **257** (2019)
10. R. Papa, M. Pirone, M. V. Nicotera, G. Urciuoli, Seasonal groundwater regime in an unsaturated pyroclastic slope, *Geotechnique* **63**, 5 (2013)
11. A. Santo, G. Di Crescenzo, G. Forte, R. Papa, M. Pirone, G. Urciuoli, Flow-type landslides in pyroclastic soils on flysch bedrock in southern Italy: the Bosco de' Preti case study, *Landslides* **15**, 1 (2018)
12. M. Pirone, R. Papa, M. V. Nicotera, G. Urciuoli, Hydraulic Behaviour of Unsaturated Pyroclastic Soil Observed at Different Scales, *Procedia Engineering* **158**, CNRIG2016 (2016)
13. M. Pirone, R. Papa, M. V. Nicotera, G. Urciuoli, In situ monitoring of the groundwater field in an unsaturated pyroclastic slope for slope stability evaluation, *Landslides* **12**, 2 (2015)
14. A. S. Dias, M. Pirone, G. Urciuoli, Calibration of TDR probes for water content measurements in partially saturated pyroclastic slope, Proceedings of UNSAT Hong Kong (2018)
15. M. Genet, A. Stokes, F. Salin, et al., The influence of cellulose content on tensile strength in tree roots, *Plant and Soil* **278** (2005)
16. G. B. Bischetti, E. A. Chiaradia, V. D'Agostino, T. Simonato, Quantifying the effect of brush layering on slope stability, *Ecol Eng.* **36**, 3 (2010)
17. R. E. Thomas, N. Pollen-Bankhead, Modeling root-reinforcement with a fiber-bundle model and Monte Carlo simulation, *Ecol Eng.* **36**, 1 (2010)

18. H. Wu, Investigation of Landslides on Prince of Wales Island , Alaska, Geotechnical Engineering Report, 5 (1976)
19. L. J. Waldron, The Shear Resistance of Root-Permeated Homogeneous and Stratified Soil1, Soil Sci Soc Am J. **41**, 5 (1977)
20. N. Pollen, A. Simon, Estimating the mechanical effects of riparian vegetation on stream bank stability using a fiber bundle model, Water Resour Res. **41**, 7 (2005)
21. M. Genet, N. Kokutse, A. Stokes, et al., Root reinforcement in plantations of *Cryptomeria japonica* D. Don: effect of tree age and stand structure on slope stability, For Ecol Manage. **256** (2008)
22. M. V. Nicotera, R. Papa, G. Urciuoli, An experimental technique for determining the hydraulic properties of unsaturated pyroclastic soils, Geotech Test J. **33**, 4 (2010)
23. M. Pirone, G. Urciuoli, Cyclical suction characteristics in unsaturated slopes, Proceedings of the International Workshop on Volcanic Rocks and Soils (2015)